

This article was downloaded by: [Dunn, Patrick F.]

On: 21 April 2010

Access details: Access Details: Free Access

Publisher Taylor & Francis

Informa Ltd Registered in England and Wales Registered Number: 1072954 Registered office: Mortimer House, 37-41 Mortimer Street, London W1T 3JH, UK



## Aerosol Science and Technology

Publication details, including instructions for authors and subscription information:

<http://www.informaworld.com/smpp/title~content=t713656376>

## A Mathematical Model of the Impact and Adhesion of Microspheres

Raymond M. Brach<sup>a</sup>; Patrick F. Dunn<sup>a</sup>

<sup>a</sup> Department of Aerospace and Mechanical Engineering, University of Notre Dame, Notre Dame, IN

First published on: 01 January 1992

**To cite this Article** Brach, Raymond M. and Dunn, Patrick F. (1992) 'A Mathematical Model of the Impact and Adhesion of Microspheres', *Aerosol Science and Technology*, 16: 1, 51 – 64, First published on: 01 January 1992 (iFirst)

**To link to this Article:** DOI: 10.1080/02786829208959537

**URL:** <http://dx.doi.org/10.1080/02786829208959537>

PLEASE SCROLL DOWN FOR ARTICLE

Full terms and conditions of use: <http://www.informaworld.com/terms-and-conditions-of-access.pdf>

This article may be used for research, teaching and private study purposes. Any substantial or systematic reproduction, re-distribution, re-selling, loan or sub-licensing, systematic supply or distribution in any form to anyone is expressly forbidden.

The publisher does not give any warranty express or implied or make any representation that the contents will be complete or accurate or up to date. The accuracy of any instructions, formulae and drug doses should be independently verified with primary sources. The publisher shall not be liable for any loss, actions, claims, proceedings, demand or costs or damages whatsoever or howsoever caused arising directly or indirectly in connection with or arising out of the use of this material.

---

# A Mathematical Model of the Impact and Adhesion of Microspheres

Raymond M. Brach and Patrick F. Dunn

*Department of Aerospace and Mechanical Engineering, University of Notre Dame, Notre Dame, IN 46556*

---

A model is presented for the low velocity planar impact of a micrometer-sized sphere (microsphere) having an arbitrary angle of approach to a surface in the presence of arbitrary contact and external forces. This model, based upon classical impact dynamics and Hertzian theories, analytically relates the velocity change of the microsphere to the physical parameters of the microsphere and the surface and to the microsphere-surface adhesion forces. The model is based upon two fundamental assumptions, namely, that the energy losses due to the process of material deformation and the process of adhesion are independent, and that the energy loss due to the adhesion process occurs

only during the rebound phase of the impact. No assumptions are made about the nature of inelastic deformations in the formulation of the model, permitting it to apply equally well to viscoelastic, elastic-plastic, or other materials or combinations thereof. The utility and accuracy of the model is assessed by comparing its predictions to experimental results. The model and the experimental data are used further to explore the relationship between the work done by the adhesion fracture force during rebound and the theoretical energy associated with the van der Waals adhesion force. The ability of the model to predict critical velocities is illustrated and discussed also.

---

## INTRODUCTION

The impact of micrometer-sized particles with surfaces occurs in a variety of situations. These include the confined flow, filtration, surface contamination, spray coating, resuspension, and dispersion of particles. Modeling of the process of particle-surface impact is complicated, primarily because it is dynamic and nonlinear. During impact, a short-duration mechanical contact is established, generating a variety of forces. For micrometer-sized particles, geometric surface and particle irregularities and molecular-level forces can be significant. In some instances, the particles may have a significant electrical charge, which introduces additional forces into the problem. All of these can occur while the particle remains within the influence of a flow field above the surface.

In this article, a model of the low velocity impact of a micrometer-sized sphere (microsphere) against a surface in the pres-

ence of arbitrary contact and noncontact (external) forces is described. The model is developed by combining concepts of contact surface adhesion energy, Hertzian mechanics of elastic spheres, and classical impact theory. Its utility is demonstrated using the microsphere-surface impact data of Wall et al. (1990). The model is considerably more general than previous ones in that it takes into account not only normal but also transverse velocity changes as well as the effects of rolling in the presence of adhesion. It is capable of handling any form of material stress-strain relationship and any type of energy dissipation mechanism.

## PREVIOUS RESEARCH

When spherical particles of most engineering materials with diameters well above 100  $\mu\text{m}$  collide with each other or with a surface at very low velocities, the collisions are

almost perfectly elastic and the ratio of the final normal velocity to the initial normal velocity tends to approach a value near unity. As the initial velocity is increased, the ratio, often called the coefficient of restitution, decreases usually monotonically and often significantly. When the particle diameters are in the range of  $1\ \mu\text{m}$ – $100\ \mu\text{m}$  and with relatively high initial velocities, the rebound velocities typically follow the same trend [Wall et al. (1990)]. But, as the initial velocities become smaller (below  $\sim 10\ \text{m/s}$ ), the rebound velocities drop off considerably, as shown in Figure 1 from the results of Dahneke (1975) for spherical particles of  $1.27\ \mu\text{m}$  diameter. For these microspheres, forces such as electrostatic and van der Waals exert an influence which plays a significant role in reducing the rebound velocity.

The adhesion force often is quantified through the use of an adhesion energy which is distributed over the contact surface of the two contacting bodies. Johnson, Kendall, and Roberts (JKR) (1971) define a surface energy due to adhesion equal to  $\gamma\pi a^2$ , hereby denoted as  $E_{\text{JKR}}$ , where  $a$  is the radius of the circular sphere-surface contact

area and  $\gamma$  is the surface energy adhesion parameter, i.e., an energy per unit contact area, which depends upon the bodies' materials and the interface properties. For given materials and particles,  $\gamma$  is considered to be a constant, at least for static contact. Bowling (1988), among others, discusses the variety of forces such as the van der Waals force that contribute to adhesion and, hence, to  $\gamma$ . Much of the basic work in the area of contact adhesion is done from the view of static or a very slowly developing interface. Roberts and Thomas (1975), for example, measure the contact force developed over a smooth rubber and glass interface which is established over periods of hours to days. In this context, the adhesion force is an "attractive" one in that an attraction takes place between the two surfaces of the interface and the adhesion "grows." Even when adhesion is viewed as a static equilibrium problem, forces are treated as attractive in nature over small separation distances of the order of molecular dimensions. Being a function of the separation distance, the van der Waals force is conservative. To account for inevitable energy losses, the view is often taken that after contact is established all of the adhesion energy required to separate a particle from a surface is lost in the separation process. Consequently, some researchers associate the van der Waals force solely with the process of separation. Among others, this view has been proposed by Billings and Wilder (1970), Clift (1985), and Hinds (1982).

The mechanism by which adhesion energy is lost can be illustrated by considering an ideal mass-spring system in which the spring is connected between the mass and a massless platform. Impact is initiated when the platform contacts a rigid, sticky surface. Following platform contact, the mass will compress the spring due to its initial kinetic energy. This will be followed by a rebound with all of the kinetic energy restored when the mass returns to the position it had at the time of initial contact. At this point the

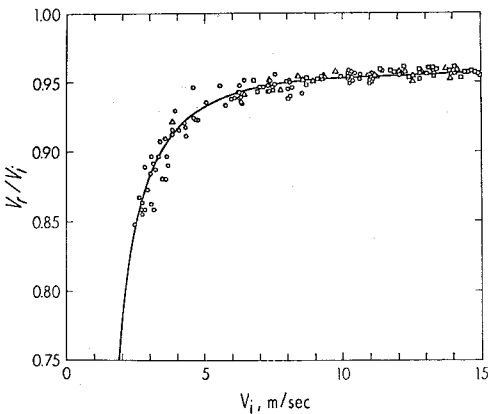


**FIGURE 1.** Ratios of final-to-initial normal velocities ( $V_r/V_i$ ) from impacts of microspheres ( $1.27\ \mu\text{m}$  diameter) against a flat surface [data of Dahneke (1975) with permission of Academic Press, copyright 1975].

platform itself, however, will not leave the surface. Because of the platform's adhesion, the spring will begin to stretch and develop a tensile force. If the strength of the adhesion bond is high, the platform will remain attached and the mass will continue to oscillate (eventually dying out in a real application). With a lower strength, however, the adhesion bond will fracture as the tensile spring force builds up, at which time the mass and spring leave the surface with a velocity less than  $v_n$  and a correspondingly lower kinetic energy. This can be compared to the "snap instability" reported by Johnson (1976). The energy loss depends upon the adhesion strength and the strain energy in the spring when the adhesion fracture occurs.

A similar mechanism is attributed to the case of microsphere impact with a flat surface. An adhesion bond is established during the approach phase of the impact and is fractured during rebound. An essential difference is that in the case of microsphere impact, the fracture process is continuous. During rebound the circular contact area is typically composed of an inner region of compressive stresses and an outer annulus of tensile adhesion stresses. A tensile adhesion force,  $F_A$  (to be discussed later) equal to  $2\pi af_0$  develops, where  $a$  is the radius of the contact circle. As the mass center moves away from the surface, the annulus shrinks and the adhesion bond progressively fractures (a process usually referred to as "peeling"). The work done,  $W_A$ , by this adhesion fracture force is part of the energy that is dissipated during rebound. Vibrations and inelastic strains in the microsphere and surface account for the remainder of the energy loss.

The above effects are taken into account from the point of view of classical impact theory, which treats an impact as a "rapid static event," ignoring vibrational motion. From an energy balance perspective, the initial kinetic energy of the particle, in addition to whatever kinetic energy is gained as

a result of the attractive (adhesion) forces, is available for rebound or dissipation. The energy associated with the rapid deformation of the particle and surface can be dissipated in a variety of ways, depending on the materials and deformation rates. The most widely encountered energy dissipative mechanisms are hysteresis, viscoelasticity, and plastic deformation. These types of energy losses occur during both the approach and rebound phases of impact. An assumption is made herein that the energy loss associated with material deformation does not interact significantly with the establishment and loss of adhesion energy. Consequently, these effects are treated independently with the adhesion energy loss occurring only during the rebound phase of the impact.

Many different analytical and experimental approaches have been used to examine and model the impact of particles with surfaces. For example, Dahneke (1971) and Loeffler (1973) report on measurements and classification of the probability of capture. They also use the conservation of energy along with a coefficient of restitution to develop an expression for the initial normal particle velocity below which rebound does not occur, a velocity which typically is referred to as the critical or capture velocity. Another approach is to adapt theories of continuum mechanics to the problem of particle-surface interaction. The most common is to use the static elastic theory of compressed spheres of Hertz [see Timoshenko and Goodier (1951)] to provide a mathematical model with a compatible stress distribution in the contact region. The corresponding forces and displacements are used in a quasi-dynamic fashion to model the impact process. Recent activity in this area centers around the analytical and experimental work of a number of researchers. They use energy conservation principles of the kinetic and potential energies during impact and the work done by various significant forces. Johnson et al. (1971) have developed a model for the stresses induced by a static adhesion

force. Johnson (1976) treats the viscoelastic problem. Rogers and Reed (1984) and Fichman and Pnueli (1985) have combined the Hertzian theory and the JKR theory for impact of elastic-plastic materials. Details of these models are discussed in Reed (1986) and Fichman and Pnueli (1986). Wall et al. (1989) report experiments in which ammonium fluorescein microspheres impacted various target materials and present a summary of how their experimental results agree with the energy balance equations and the elastic-plastic Hertzian theories. Through the introduction of strain rate effects, they show quite good agreement with the Rogers and Reed theory but claim that the adhesion force parameters are not yet realistic.

A fresh approach to the impact process is taken in this article that stems from recent work of Brach (1991a, b) on the classical impact problem. A departure from previous researchers is to associate the coefficient of restitution with the mechanical energy lost in the normal deformation of the sphere and surface, exclusive of the adhesion energy. A new feature is the introduction of the effects of tangential and rotational motions of the microsphere. This permits accounting for the energy lost due to transverse forces such as friction. The equations are also developed to include the effects of adhesion for rolling during impact such as observed by Roberts and Thomas (1975) in static experiments. As done by many others, the classical Hertzian model of the forces, stresses and deformation of an elastic sphere is used. Transverse elastic deformation of spheres was analyzed by Mindlin and Deresiewicz (1953) and has been observed in discs during impact by Maw et al. (1977). These effects can be included in the impact equations as shown by Brach (1991b) but are not herein.

A considerable amount of effort of recent researchers has been concentrated on developing an impact theory for spheres made of elastic-plastic materials. The equations in this article apply to these materials but are not restricted to them. The point of view is

taken that other classes of materials such as viscoelastic (polymers and elastomers) and brittle (fly ash) are equally important and a more general theory is sought. In addition, the elastic-plastic theories that have developed include a ring of infinite tensile stresses on the outer edge of the contact circle during both approach and rebound, even for very low velocities. The plastic deformation corresponding to these large stresses apparently never has been observed experimentally, opening the possibility that this model may be somewhat unrealistic. Furthermore, according to Timoshenko and Goodier (1951), compressive plastic deformation in ductile spheres takes place, at least initially, beneath the surface, and at very low velocities can cause residual stresses but is not likely to produce significant changes in spherical shape. For this reason, permanent deformation per se does not play a role in the following model, although any corresponding energy loss is considered.

## IMPACT MODEL

### Classical Impact Theory

In the absence of transverse spin (roll spin) or spin about the vertical axis (yaw spin) the impact of a sphere with a surface can be viewed as a planar mechanics problem. Some of the pertinent assumptions for this problem are as follows:

- The particle need only be nearly spherical provided it has a spherical shape in the contact region and its mass center lies on or very near the perpendicular from the contact surface.
- The particle retains its original shape following impact.
- At lower initial velocities (when capture is likely) the energy loss associated with material deformation is small but not necessarily negligible.
- Adhesive losses are significant only during the rebound phase of the impact and correspond to a fracture of the

adhesion bond at the periphery of the receding contact surface.

- The processes of adhesion energy loss and deformation energy loss are independent.

Figure 2 shows a sphere of radius  $r$ , a normal and tangential  $n - t$  coordinate system and the impulse components of the forces felt by the sphere and which are distributed over the contact surface and contact duration. Throughout this article, upper-case  $V$ 's refer to final velocities at the end of a time interval, and lower-case  $v$ 's refer to initial velocities at the beginning of a time interval. The approach phase of the impact is from the time of initiation of the contact,  $\tau_1$ , to the time  $\bar{\tau}$ , at which the mass center of the deformed sphere comes to rest. The rebound phase is from  $\bar{\tau}$  to the time  $\tau_2$  when contact ends. For the approach phase in the normal direction, Newton's laws in impulse and momentum form give

$$-mv_n = P_D^A + P_E^A. \tag{1}$$

Here,  $m$  is the mass of the particle,  $v_n$  is the initial normal velocity ( $v_n < 0$ ),  $P_D^A$  is the approach-phase impulse corresponding to the

forces of deformation of the sphere and surface, and  $P_E^A$  is the approach-phase impulse of any significant external forces (such as those resulting from electrostatic attraction or repulsion). For the rebound phase, the corresponding expression is

$$mV_n = P_D^R + P_E^R - P_A, \tag{2}$$

where  $V_n$  is the final rebound velocity at  $\tau_2$  and  $P_A$  is the impulse of the adhesion fracture force. For the entire contact duration,

$$mV_n - mv_n = P_n = P_D + P_E - P_A, \tag{3}$$

where  $P_n$  is the resultant normal impulse. In the tangential direction for the entire contact duration,

$$m(V_t - v_t) = P_t, \tag{4}$$

where  $P_t$  is the resultant tangential impulse. Over the full duration, for rotational motion, the change in angular momentum must equal the impulse moments; that is,

$$I(\Omega - \omega) = M - rP_t \tag{5}$$

where  $I$  is the particle's inertia,  $\omega$  its angular (rotational) velocity before impact and  $\Omega$  after,  $r$  is its radius, and  $M$  is the impulse of the surface moment.

In Brach (1991b), different forms for the coefficient of restitution,  $R$ , are discussed. A kinematic definition is used here where  $R$  is defined as

$$R = P_D^R / P_D^A. \tag{6}$$

Two other coefficients are defined. The first is the impulse ratio  $\mu$ , where

$$\mu = P_t / P_n. \tag{7}$$

Note that  $\mu$  generally is *not* a coefficient of friction; it is a ratio of impulses, not a ratio of forces. In some special cases (such as for sliding throughout the entire contact duration),  $\mu$  can be equal to the coefficient of friction. For further clarification, see Brach (1991a). A third coefficient, the moment coefficient,  $e_m$  is defined as

$$e_m M / I = (1 + e_m) \Omega. \tag{8}$$

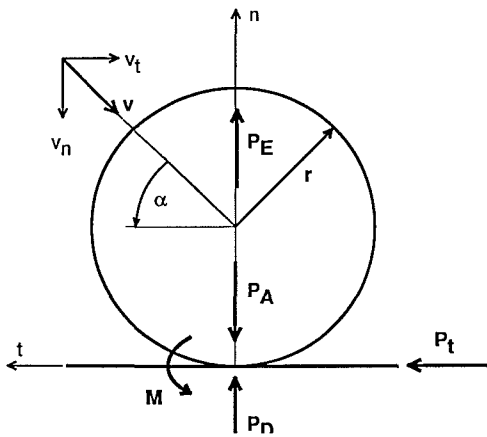


FIGURE 2. Diagram of a sphere in contact with a flat surface showing impulse components, velocity components, and the normal and tangential coordinate system.

Downloaded By: [Dunn, Patrick F.] At: 15:10 21 April 2010

Note that  $e_m$  has an analogous purpose for angular motion as the coefficient of restitution  $R$  for motion normal to the contact surface. From Eq. 8, it is clear that for  $e_m = 0$ ,  $\Omega = 0$ , which represents a totally inelastic rotational impact. For  $e_m = -1$ , however,  $M = 0$  and is the case where no rotational effects due to the contact force exist. The coefficient  $e_m$  is bounded by  $-1 \leq e_m \leq 1$  and can be used to simulate adhesion energy loss in a sphere that rolls during impact, such as was observed for nonimpact adhesion by Roberts and Thomas (1975).

Equations 1–8 represent a complete set of system equations for the planar impact problem. If the initial velocities, coefficients, and external impulses are assumed known, the unknowns are  $V_n$ ,  $V_t$ ,  $\Omega$ ,  $P_D^R$ ,  $P_D^A$ ,  $P_n$ ,  $P_t$ , and  $M$ . All of the solution equations for these unknowns could be written here, but only those needed will be introduced. At this point attention is turned to the impulse,  $P_A$ , of the adhesion force. The work done by an impulse is equal to its product with the average velocity along its direction of application. For the work of the resultant normal impulse,  $P_n$ , this gives

$$W_n = P_n(v_n + V_n)/2. \quad (9)$$

The final normal velocity is found using Eqs. 1, 2, and 6; this gives

$$V_n = -Rv_n - P_A/m - (P_E^R - RP_E^A)/m. \quad (10)$$

Although they are easily carried through the full analysis, at this point the arbitrary, external impulses  $P_E^R$  and  $P_E^A$  are assumed to be zero. Substitution of  $V_n$  from Eq. 10 into Eq. 9 yields an expression for  $P_A$  in terms of the energy lost through deformation,  $(1 - R^2)mv_n^2/2$ , and the work done,  $W_A$ , in overcoming the adhesion energy (note that  $W_A < 0$ ). This is

$$P_A = -mRv_n \times \left[ 1 - (1 + 2W_A/R^2mv_n^2)^{1/2} \right]. \quad (11)$$

At this point the unknown final velocities can be expressed in terms of the initial velocities, the coefficients, and the work of adhesion. For example,

$$V_n = -Rv_n(1 + 2W_A/R^2mv_n^2)^{1/2}, \quad (12)$$

$$V_t = v_t - \mu v_n(1 + R) \times (1 + 2W_A/R^2mv_n^2)^{1/2}, \quad (13)$$

and

$$\Omega = -e_m\omega - e_m\mu \times \left[ 1 + (1 + 2W_A/R^2mv_n^2)^{1/2} \right] mrv_n/I. \quad (14)$$

The impulse components  $P_n$  and  $P_t$  can be found by using these expressions for the final velocities and Eqs. 3 and 4.

The choice of appropriate values of the coefficients  $R$ ,  $e_m$ , and  $\mu$  needs some discussion. Because  $R$  is defined as the restitution coefficient in the absence of adhesion (and electrostatic) effects (when the approach and rebound components of  $P_A$  and  $P_E$  are negligible compared to the corresponding  $P_D$  components), its behavior is expected to follow usual trends of decreasing with increasing  $v_n$ . In the following, this is approximated by

$$R = k / (k + |v_n|^p), \quad (15)$$

where the appropriate values of constants  $k$  and  $p$  can be found from experimental data. Of course, other appropriate expressions could be used in place of Eq. 15; for very low initial velocities, a constant value such as  $R \approx 1$  could be used. The equations for the relationship  $R(v_n)$  do not have to be experimental ones, but they can be theoretical. For example, Wall et al. (1989) discuss the elastic-plastic model of Rogers and Reed (1984) and indicate that it provides good results if modified to take into account plastic strain rate effects. Based on this model,  $R = [1 - K_p/K_i]^{1/2}$ , where  $K_i$  is the initial kinetic energy and  $K_p$  the energy lost due to plastic deformation, with  $K_p$  depending

on the yield strength, initial kinetic energy, elastic constants, etc. Another example by Brach (1991a) shows that viscous damping can be modeled (if appropriate) using  $R = \exp[-\pi \zeta / (1 - \zeta^2)^{1/2}]$ , where  $\zeta$  is the damping ratio encountered in linear vibration theory. Such analytical expressions for  $R$  can be used as alternatives for Eq. 15, which illustrates an important feature of the mathematical model presented herein, namely, its generality.

Little or no theoretical information or experimental data is available from the literature on the impact of microspheres that can provide information for the moment coefficient  $e_m$ . This phenomenon is relegated to future research, and at this point a value of  $-1$  is used which corresponds to the assumption that the moment impulse  $M = 0$ . To simplify the model further, the rotational energy of the pertinent range of particle sizes is assumed to be insignificant and a point mass impact model is developed (which implies that rotational velocities are all zero).

Finally, appropriate values of the impulse ratio  $\mu$  must be determined. Most intended applications are for low velocity impacts (including small spin velocities). In particular, a primary interest here lies in those conditions where the particle attaches itself to the surface. In this case it is reasonable to assume that friction or any other tangential force (such as indentation for a hard particle and soft surface) is sufficiently large to cause the particle's tangential contact velocity to become zero during the impact. From Eq. 13, zero final tangential velocity for a particle requires that the impulse ratio be

$$\begin{aligned} \mu &= \mu_0 \\ &= \eta / [1 + (R^2 + 2W_A / mv_n^2)]^{1/2}, \quad (16) \end{aligned}$$

where  $\eta = v_t / v_n = 1 / \tan \alpha$  (see Figure 2).

Note that for a normal impact,  $v_t = 0$ ,  $\mu_0 = 0$ , and by Eq. 7,  $P_t = 0$ . That is, no tangential impulse is possible in this case. If, as discussed by Brach (1991a), in the presence of low values of friction, the final

tangential velocity is not zero, then  $\mu$  in Eq. 13 is replaced by the value of the coefficient of friction.

Another important equation expresses the kinetic energy loss of the microsphere that results from impact. The energy loss  $T_L$  is found simply by subtracting the final kinetic energy of the particle from its initial. This gives

$$\begin{aligned} T_L &= \frac{1}{2} m (V_n^2 - v_n^2) = -W_A + \frac{1}{2} m v_n^2 \\ &\quad \times \left[ (1 - R^2) + \eta^2 \frac{\mu}{\mu_0} \left( 2 - \frac{\mu}{\mu_0} \right) \right]. \quad (17) \end{aligned}$$

For the special case of normal impact this yields

$$W_A = \frac{1}{2} m v_n^2 [(V_n^2 / v_n^2) - R^2], \quad (18)$$

which implies that the work of adhesion can be determined using Eq. 15 (or a suitable alternative), directly from the measurements of  $v_n$  and  $V_n$ .

### Hertzian Theory

As reasoned by Brach and Dunn (1991) and discussed above, the adhesion bond established during the approach phase is overcome or fractured during the rebound phase through a force distributed over the periphery of the receding circular contact area. An idealized line force is chosen such that when the radius of the contact area is  $a$ , the force is  $F_A = 2\pi a f_0$ , where  $f_0$  is the circumferential "tension" of the adhesion fracture force with units of  $N/m$ . Up to this point no assumptions have been made about the nature of the microsphere or surface material. From here on, it is assumed only that Hertzian theory can be used to approximate its deformation. The Hertzian equations of the elastic behavior of a sphere in contact with an elastic surface as presented by Timoshenko and Goodier (1951) are now



used to determine the work,  $W_A$ , corresponding to the fracture of the adhesion bond.

The work done by  $F_A$  during rebound is

$$\begin{aligned} W_A &= -4\pi f_0 a_m^3 / 3r \\ &= -2a_m^2 F_A / 3r, \end{aligned} \quad (19)$$

where  $a_m$  is the maximum contact area radius. From Hertzian theory the maximum contact area radius is

$$a_m = \left[ \frac{15\pi}{8} (k_1 + k_2) r^2 \frac{1}{2} m v_n^2 \right]^{1/5}, \quad (20)$$

where  $k_i = (1 - \nu_i^2) / \pi E_i$  and  $\nu_i$  and  $E_i$  are Poisson's ratio and Young's modulus for the particle and surface materials. Now, if the work of the adhesion force is set equal to the JKR surface adhesion energy,  $E_{JKR}$ , then, using Eq. 19 and the definition of  $F_A$ , the surface energy adhesion parameter becomes

$$\gamma = 2F_A / 3\pi r. \quad (21)$$

This consequently yields

$$W_A = - \left[ \frac{5}{4} \rho \pi^{9/2} (k_1 + k_2) \right]^{2/5} \gamma r^2 |v_n|^{4/5}, \quad (22)$$

where  $\rho$  is the particle's material density. Equation 22 can be used to eliminate  $W_A$  from previous equations to determine the particle's rebound velocities, the energy loss, and the critical velocity in the presence of an adhesion force, coefficient of restitution, and tangential effects as characterized by the respective parameters  $\gamma$ ,  $R$ , and  $\mu$ . Furthermore, using Eqs. 15, 18, and 22, the surface adhesion energy parameter  $\gamma$  can be found directly for the case of normal impact experiments in which  $v_n$  and  $V_n$  are measured.

## APPLICATION OF THE THEORY

### The Surface Adhesion Energy

The data for normal impacts acquired by Wall et al. (1989) for ammonium fluorescein microspheres are used here to illustrate some

of the features of the model. In their experiments, ammonium fluorescein ( $\text{NH}_4\text{Fl}$ ) microspheres of 2.58  $\mu\text{m}$ , 3.44  $\mu\text{m}$ , 4.90  $\mu\text{m}$ , and 6.89  $\mu\text{m}$  diameter impacted normally against smooth, flat surfaces made of molybdenum, silicon, mica, and Tedlar (polyvinyl-fluoride) over an initial velocity range of approximately 3–120 m/s. The data corresponding to 4.90  $\mu\text{m}$  diameter spheres and the molybdenum target are the most numerous and are used for illustration. The values of the material properties and impact parameters for one case in this data set are presented in Table 1 for illustrative purposes.

For the data, which include three target surfaces (mica, molybdenum, and silicon), the least squares fit of Eq. 15 produces the equation

$$R = 45.3 / \left( 45.3 + |v_n|^{0.718} \right) \quad (23)$$

with a correlation coefficient value of 0.969 for 19 samples, which corresponds to a 99.9% probability of fit (Taylor 1982). This can be used in the above equations to provide a means of predicting the final rebound velocities. For the 4.90  $\mu\text{m}$  diameter microspheres and a molybdenum target, Figure 3 shows the predicted and experimental final-to-initial normal velocity ratios over the range of experimental initial normal velocities, with obvious good agreement between the two.

Based on the low velocity data, i.e., less than 10 m/s, Brach and Dunn (1991) have already shown that the surface energy adhesion parameter  $\gamma$  appears to be dependent on the initial normal velocity. This can be examined further by comparing the  $\gamma$ 's for all target materials and particle diameters in this velocity range, as shown in Figure 4. The data are described best by the simple relation

$$\gamma = 0.34 |v_n|^{1/2}, \quad (24)$$

which is the solid line plotted in Figure 4. The quantity  $\gamma$  usually is considered to be a constant. The experimental data as reflected in Eq. 24 show otherwise. The significance

**TABLE 1.** Impact of an Ammonium Fluorescein Sphere against a Molybdenum Surface

Ammonium fluorescein sphere		Impact mechanics	
$\rho$ , density	$1.35 \times 10^3 \text{ kg/m}^3$	$v_n$ , initial velocity <sup>2</sup>	8.23 m/s
$E$ , Young's modulus	$1.2 \times 10^9 \text{ N/m}^2$	$V_n$ , final velocity <sup>2</sup>	6.50 m/s
$\nu$ , Poisson's ratio	0.33	$V_n/v_n$ , velocity ratio <sup>2</sup>	0.790
$n$ , index of refraction	1.56	$\alpha_m$ , elastic displacement <sup>1</sup>	$9.12 \times 10^{-8} \text{ m}$
$\epsilon$ , dielectric constant	2.55	$a_m$ , contact radius <sup>1</sup>	$4.73 \times 10^{-7} \text{ m}$
$d$ , diameter	$4.90 \times 10^{-6} \text{ m}$	Hertzian contact force (max) <sup>1</sup>	$7.72 \times 10^{-5} \text{ N}$
$m$ , mass	$8.32 \times 10^{-14} \text{ kg}$	$F_A$ , adhesive force (max) <sup>1,3</sup>	$9.36 \times 10^{-6} \text{ N}$
		$\tau$ , contact duration <sup>1</sup>	$3.26 \times 10^{-8} \text{ s}$
		$R$ , coefficient of restitution <sup>2,3</sup>	0.909
		$T_i$ , initial kinetic energy <sup>2</sup>	$2.82 \times 10^{-12} \text{ J}$
		$T_f$ , final kinetic energy <sup>2</sup>	$1.76 \times 10^{-12} \text{ J} (62.4\% T_i)$
		$(1-R^2)mv_n^2/2$ , deformation energy <sup>2,3</sup>	$4.90 \times 10^{-13} \text{ J} (17.4\% T_i)$
		$W_A$ , work of adhesion fracture <sup>1,2</sup>	$5.69 \times 10^{-13} \text{ J} (20.2\% T_i)$
		$E_h$ , van der Waals energy (max) <sup>1,3</sup>	$1.64 \times 10^{-12} \text{ J} (58.2\% T_i)$
<b>Molybdenum surface</b>			
$E$ , Young's modulus	$3.2 \times 10^{11} \text{ N/m}^2$		
$\nu$ , Poisson's ratio	0.30		
$n$ , index of refraction	3.56		
$\epsilon$ , dielectric constant	$\infty$		
$z_0$ , intermolecular distance	$4 \text{ \AA}$		
$h$ , Lifschitz-van der Waals constant	4.56		

<sup>1</sup>Hertzian Theory  
<sup>2</sup>Experimental  
<sup>3</sup>Theoretical

of this is unknown at present and could reflect a defect in the model or an incorrect view of  $\gamma$  with respect to the process of adhesion. This topic is not pursued here.

**Critical Velocity**

The critical velocity is the initial velocity for which  $V_n^2 + V_t^2 = 0$ . It is conveniently

expressed as

$$v_c^2 = -\frac{1 + \eta^2}{R^2} \frac{2W_A}{m} \tag{25}$$

However, when expressed in this form,  $v_c$  is contained implicitly on the right-hand side

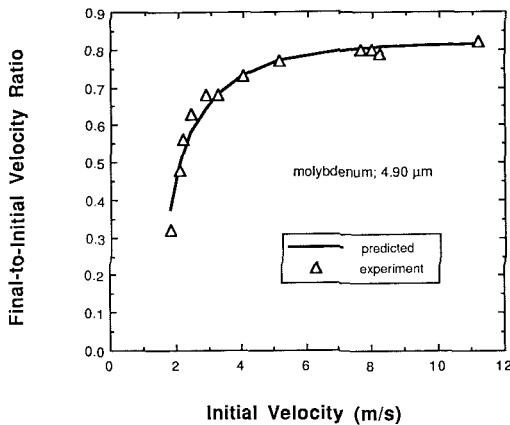


**FIGURE 3.** The final-to-initial normal velocity ratios for  $4.90 \mu\text{m}$  diameter  $\text{NH}_4\text{Fl}$  spheres against a molybdenum target from the data of Wall et al. (1990).

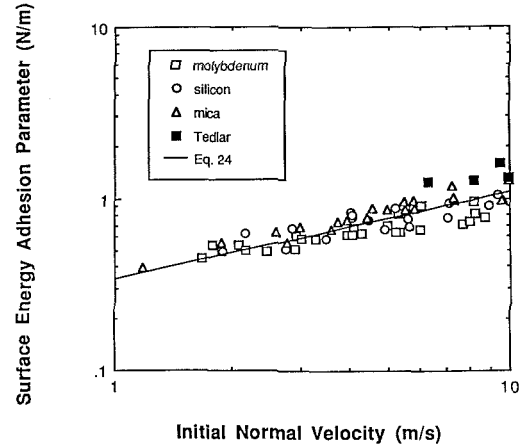


**FIGURE 4.** Values of the surface energy adhesion parameter from the data of Wall et al. (1990) for four diameters of  $\text{NH}_4\text{Fl}$  spheres and four target materials. The solid curve is calculated from Eq. 24.

of this equation. This is because both  $W_A$  and  $R$ , as specified by Eqs. 22–24, are functions of  $v_n$ , which equals  $v_c$  for this case.

Proceeding along these lines, Eqs. 22–24 can be applied to the case when  $v_n = v_c$  and substituted into Eq. 25 and rearranged to yield an expression for the critical velocity

$$v_c = \left[ \frac{H(1 + \eta^2)}{rR^2} \right]^{10/7}, \quad (26)$$

where  $H = 0.51 [5\pi^2(k_1 + k_2)/4\rho^{3/2}]^{2/5}$ , which is a function solely of material constants. This equation still remains an equation that is transcendental in  $v_c$  because  $R$  is evaluated at  $v_c$  and is empirically based because of the use of Eq. 23. Equation 26 is solved best by iteration, four solution points of which are presented in Figure 5 for the case of a molybdenum target. The values of the critical velocities for mica and silicon were found all to be within approximately 2% of the molybdenum values for each of the four diameters examined and therefore are represented by the same four points shown in Figure 5. Those for the Tedlar surface are not presented because no high

velocity data was available to determine an appropriate fit to Eq. 15 that would yield  $R$  as a function of  $v_n$ . Also shown are the solutions for  $v_c$  using Eq. 26, in which the values for  $\eta$  and  $R$  are fixed and assumed not to be a function of  $v_c$ . The solution curves for  $\eta = 0$  and  $R = 1$  and 0.9 bound the transcendental equation solutions, where for normal initial impact  $R$  was found to range from 0.952 to 0.983 over the critical velocity range from 3.14–0.70 m/s. This implies that, for application to the subject experiments,  $R$  can be assumed to be a constant without introducing substantial error when determining the critical velocities. Further, it can be seen that oblique incidence impacts may yield critical velocities approximately a factor of 6 higher than their normal incidence counterparts for the same  $R$  value. This is because of the additional energy loss due to friction for oblique impacts. A reduction in  $R$  for the same angle of incidence also leads to an increase in the critical velocity because of the inherent increase in kinetic energy loss upon impact.

The Eq. 26 solution results shown in the figure also closely match to within  $\sim 20\%$  those reported by Wall et al. (1990) that were determined for the molybdenum, silicon, and mica cases in a different manner but using the same data. The slope of a line through the four Eq. 26 solution points equals  $-1.53$ , which compares quite favorably with those of Wall et al. (1990), which equalled  $-1.22$ ,  $-1.40$ , and  $-1.58$  for the molybdenum, silicon, and mica cases, respectively. These slopes are comparable also to those of several other investigators cited by Wall et al. (1990).

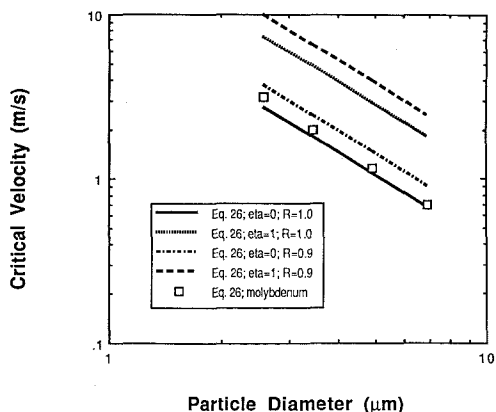


**FIGURE 5.** Critical velocities for the normal and oblique impacts of  $\text{NH}_4\text{F}$  spheres against a molybdenum target surface for various  $R$  and  $\eta$ . These parameters represent the energy loss due to material deformation and angle of incidence, respectively.

## Adhesion Force

Further insight into the role that the adhesion force plays can be gained by considering the forces that arise as a result of deformation which must be overcome if the microsphere is to rebound from the surface. These forces (in  $N$ ), whose sum is denoted

by  $F_\Sigma$ , can include the van der Waals force acting over the contact area  $F_{vdW}$ , the capillary force resulting from the presence of liquid along the periphery of contact  $F_{cap}$ , the gravitational force  $F_g$ , and two electrostatic forces  $F_i$  and  $F_{cp}$ , originating from the image and contact potential forces, respectively. [These forces are described collectively by Bowling (1988) and Hinds (1982).] These considerations imply

$$F_\Sigma = F_{vdW} + F_{cap} + F_g + F_i + F_{cp}, \quad (28)$$

where

$$F_{vdW} = ha_m^2 / 8\pi z^3, \quad (29)$$

$$F_{cap} = [3.75 \times 10^{-6} + 3.38 \times 10^{-8} \%RH] r, \quad (30)$$

$$F_g = \rho g 4\pi r^3 / 3, \quad (31)$$

$$F_i = q^2 / 16\pi \epsilon_r \epsilon_0 r^2, \quad (32)$$

and

$$F_{cp} = \pi \epsilon_0 r \Phi^2 / z. \quad (33)$$

In these expressions,  $h$  is the Lifshitz-van der Waals constant, which depends upon the dielectric constants of the materials involved [see Rumpf (1990) or Bowling (1988)],  $z$  is the atomic separation or adhesion distance that occurs between the materials during deformation,  $\%RH$  is the relative humidity in percent,  $q$  the particle charge,  $\epsilon_r$  the relative dielectric constant (1.00059 for air),  $\epsilon_0$  the permittivity of free space ( $8.85 \times 10^{-12}$  F/m), and  $\Phi$  the contact potential difference. This potential difference arises from the difference in the thermionic work functions of the two materials. The expression for  $F_{cap}$  is empirical, as presented by Hinds (1982). An estimate for  $q$  can be made for the case when a charge is not deliberately imposed upon the particle by assuming an equilibrium (Boltzmann) charge state, where  $q = \bar{n}e$ , with  $\bar{n}$ , the average number of either positive or negative charges, approximated by the empirical expression  $\bar{n} = 3350 r^{1/2}$  and  $e = 1.6 \times$

$10^{-19}$  C [Hinds (1982)]. The expression for the electrostatic image force implicitly assumes no charge loss during impact, i.e., the particle acts as a dielectric during the duration of contact, which was of the order of  $\sim 1 \mu s$  in Wall's experiments.

As shown by Bowling (1988), under typical conditions, the van der Waals force is the dominant force for microspheres. Substitution of the parameter values that are appropriate for the subject experiments ( $h = 1$  eV,  $z = 4 \times 10^{-10}$  m, and  $\Phi = 0.5$  V) yields the same conclusion. For these calculations, the value of the Lifshitz-van der Waals constant chosen was the average of the range of values presented by Bowling (1988) for a polymer particle collision with a polymer or metallic surface. Reported values for  $h$  for various materials range from approximately 0.1–10 eV [Bowling (1988)]. The value of  $\Phi$  is a typical maximum value [Bowling (1988)] and that of  $z$  is that typically chosen as a representative value [Dahneke (1972)]. Subject to these conditions, the magnitude of the van der Waals force ranges from approximately 1–10  $\mu N$ . Over the entire range of experimental conditions, this is at least one to two orders of magnitude greater than the capillary force and several orders of magnitude greater than the electrostatic and gravitational forces. Hence, for the subject experiments, the van der Waals force dominates such that  $F_\Sigma$  can be approximated by  $F_{vdW}$ .

For the static case of a microsphere resting on a flat surface, the work,  $W_A$ , required to fracture the adhesion bond equals the energy resulting from the van der Waals attraction,  $E_h$ , assuming all other forces contributing to  $F_\Sigma$  remain negligible. For the dynamic case of microsphere impact, however, the microsphere's initial kinetic energy, in addition to the energy acquired during the approach phase by the van der Waals attraction, is available to overcome adhesion during rebound. Only a fraction of  $E_h$ , i.e.,  $W_A/E_h$ , is found from the experiments to be necessary to overcome adhesion.

The energy acquired during the approach phase from the van der Waals attraction for this case is

$$E_h = 2a_m^2 F_{vdW} / 3r = ha_m^4 / 12\pi rz^3. \quad (34)$$

Substitution of the expression for  $a_m$  (Eq. 20) into this equation reveals the relationship between  $E_h$ ,  $v_n$ , and  $r$ ; that is,

$$E_h = (h/12\pi^2 z^3) \times [5\pi^2 \rho(k_1 + k_2)/4]^{4/5} r^3 |v_n|^{8/5}. \quad (35)$$

In this expression,  $h$ ,  $r$ ,  $\rho$ ,  $k_1$ , and  $k_2$  are fundamental or calculated material and geometric constants. The adhesion distance  $z$  is also assumed to be constant. Using this expression and that for  $W_A$  (Eq. 22) with Eq. 24 reveals that the ratio  $W_A/E_h$  varies inversely with the product  $r|v_n|^{0.3}$ . This implies that, for a particle of a given size, as the initial normal velocity is increased, the fraction of the energy required to fracture the adhesion bond decreases. Furthermore, for a given initial normal velocity, this fraction decreases with increasing particle size. An empirical evaluation of this ratio, however, requires that the values of  $h$  be known for each of the combinations of materials and medium considered.

The specific values for the Lifshitz-van der Waals constant for each of the four combinations of materials and medium examined in Wall's experiments are not available in the literature. The Lifshitz-van der Waals constant, found directly from the Hamaker constant  $A$ , where  $h = 4\pi A/3$ , can be determined in a straightforward manner for various combinations of nonconductors, as described by Israelachvili (1985). This, however, requires a knowledge of the medium's and materials' dielectric permittivities and refractive indices, which are wavelength dependent. For situations involving conductors, the method to determine  $A$  is more complex: a wavelength-dependent integral solution is required.

Consequently, for the present comparison with experiment, the values of  $h$  for the combinations of  $\text{NH}_4\text{FI}$ -air-mica and  $\text{NH}_4\text{FI}$ -air-Tedlar were determined using Israelachvili's approach and found to be equal to 1.71 and 1.43 eV, respectively, assuming the properties of  $\text{NH}_4\text{FI}$  to be those of polystyrene. The values of  $h$  for the combinations of  $\text{NH}_4\text{FI}$ -air-molybdenum and  $\text{NH}_4\text{FI}$ -air-silicon were estimated for each combination as arithmetic averages of the  $h$ 's for the interactions of each of the two component materials with themselves across air and were found to be equal to 4.56 and 4.42 eV, respectively.

With these values in hand, the fraction of the energy acquired by the van der Waals attraction that is required to fracture the adhesion bond during impact can be evaluated for all of the 16 cases examined by Wall et al. (1990). The results of this comparison are displayed in Figure 6. It is apparent for each of the four target materials that a smaller percentage of  $E_h$  is required to fracture the adhesion bond with increasing values of  $E_h$ , which also corresponds to increasing initial normal velocity. For the two "softer" target materials having the lowest elastic modulus values (Tedlar and mica), this percentage ranges from approximately 70–80% at the lowest initial normal velocity ( $\sim 2$  m/s) to approximately 25% at the highest velocity ( $\sim 10$  m/s). For the other two "harder" target materials, this percentage is reduced to the range of approximately 25% at the lowest velocity to approximately 5% at the highest velocity. Further, for the same initial normal velocity, as shown in the Figure 6, the percentage of  $E_h$  decreases with increasing values of the elastic modulus of the target material. Finally, the effect of the size of the microsphere for a given material is not apparent in the figure. This is primarily because the large range of values presented in the figure and the relatively small difference in diameters studied in the subject experiments masked this dependency, which was predicted and described previously.

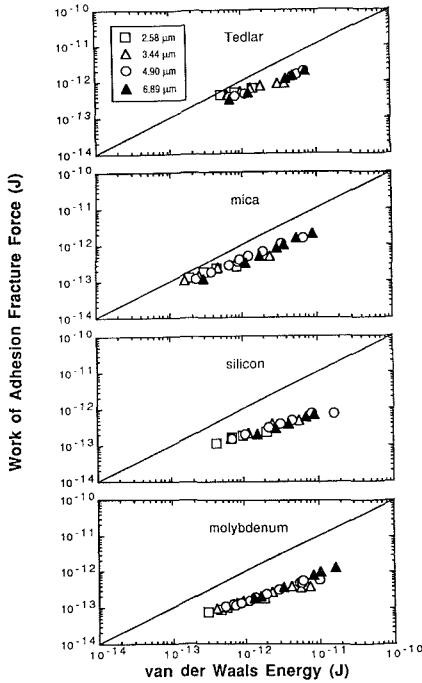


**FIGURE 6.** The work,  $W_A$ , required to fracture the adhesion bond versus the energy,  $E_h$ , acquired by the van der Waals attraction for the four different diameter microsphere impact cases of Wall et al. (1990).

## SUMMARY AND CONCLUSIONS

A model for the low velocity impact of microspheres with surfaces based upon classical impact dynamics and Hertzian theories was developed and presented. The model is broadly applicable to rounded particles undergoing oblique impact with a relatively massive surface. Any system of surface forces and moments can be treated. A unique feature of the model is that energy losses due to material deformation are included through the use of the coefficient of restitution, whereas adhesion energy losses are treated independently through use of the work  $W_A$  of the adhesion fracture force  $F_A$ .

The model's utility and accuracy were demonstrated using the experimental data of Wall et al. (1990), which involved the dynamics of four different diameter ammonium fluorescein particles impacting molyb-

denum, silicon, mica and Tedlar surfaces. With the coefficient of restitution and the Johnson-Kendall-Roberts (JKR) surface energy adhesion parameter fit to the experimental data, the model predicted the measured particle dynamics with high accuracy.

Using the model to analyze the experimental data rather than a predictive technique permitted the examination of the behavior of the JKR surface energy adhesion parameter. It was found that for all four surface materials and four particle diameters, the JKR parameter  $\gamma$  was proportional to the square root of the initial normal velocity of the particle (with an exceptionally high and statistically significant correlation coefficient). If  $\gamma$  is presumed to be a constant, this implies that some feature of the model may be incorrect. For example,  $a_m$  might be different from that predicted by the Hertzian model. If so, a better model for computing more realistic values of  $a_m$  is required. A study of this nature is planned for future research. The ability of the model to predict critical velocities accurately was also demonstrated.

A review was presented of the variety of forces that arise during the contact of micrometer-sized particles with a surface. For the application corresponding to Wall's data, the van der Waals force is dominant. Again, the characteristics of the impact model permitted the examination of the relationship between the work required to fracture the adhesion bond and the energy acquired from the van der Waals attraction. The comparison revealed that for impact not all of the adhesion energy is lost during separation. Here, a smaller fraction of the van der Waals energy is needed to fracture the adhesion bond during rebound with increasing initial velocity for a given target material and with increasing elastic modulus for different target materials at the same initial velocity.

The model is also capable of treating oblique impacts, where energy losses due to friction are encountered. However, its accuracy for such cases cannot be assessed at

present because of the scarcity of data in this area. For a given initial particle velocity, the normal and tangential components depend on the angle of approach,  $\alpha$ , that is,  $v_n = v_0 \cos \alpha$  and  $v_t = v_0 \sin \alpha$ . The introduction of these into Eqs. 16 and 17 shows that the resultant effect is not a simple one. The nature of rebound depends not only on the usual effects (restitution and adhesion), as already shown, but also on the approach angle, the friction coefficient, and its effect on the impulse ratio (which depends upon whether or not sliding ends before contact ceases). Such complexity is illustrated in the data of Wang and John (1988), where some cases show that the capture rate increases then decreases as  $\alpha$  changes from normal to grazing impact. Clearly, additional study of this complex problem is necessary, with the ultimate goal of an experimentally verified model that considers tangential effects as well as particle and target electrical charge.

The authors acknowledge the assistance of Drs. Steven Wall and Walter John, who have graciously provided us with a tabulation of their data as well as answering several questions concerning their experiments and analysis. The information and assistance obtained in a conversation with Professor K. L. Johnson was also helpful and is gratefully acknowledged.

## REFERENCES

- Billings, C. E., and Wilder, J. (1970). *Handbook of Fabric Filter Technology, Vol. 1, Fabric Filter Systems Study*, U.S. Dept. H.E.W., GCA-TR-70-17-G.
- Bowling, R. A. (1988). In *Particle Surfaces 1*, (K. L. Mittal, Ed.), Plenum Press, New York.
- Brach, R. M. (1991a). *Mechanical Impact Dynamics*, John Wiley, New York.
- Brach, R. M. (1991b). In *Computational Aspects of Impact and Penetration*, (R. F. Kulak and L. Schwer, eds.), Elme Press, Lausanne, Switzerland.
- Brach, R. M., and Dunn, P. F. (1991). In *Fluids Engineering Division Vol. 113, Forum on Micro Fluid Mechanics 1991* (L. M. Trefethen, ed.), The American Society of Mechanical Engineers, New York, pp. 11–16.
- Clift, R. (1985). I. CHEM. E. Symposium Series No. 91, Birmingham, UK, pp. 27–43.
- Dahneke, B. (1971). *J. Colloid Interface Sci.* 37:342–353.
- Dahneke, B. (1972). *J. Colloid Interface Sci.* 40:1–13.
- Dahneke, B. (1975). *J. Colloid Interface Sci.* 51:58–65.
- Fichman, M., and Pnueli, D. (1985). *J. Appl. Mech.* 52:105–108.
- Fichman, M., and Pnueli, D. (1986). *J. Appl. Mech.* 53:230.
- Hinds, W. C. (1982). *Aerosol Technology*, John Wiley, New York.
- Israelachvili, J. N. (1985). *Intermolecular and Surface Forces*, Academic Press, New York.
- Johnson, K. L. (1976). In *Theoretical and Applied Mechanics*, (W. T. Koiter, ed.), North-Holland, Delft.
- Johnson, K. L., Kendall, K., and Roberts, A. D. (1971). *Proc. Royal Soc. London* 324:301–313.
- Loeffler, F. (1973). *Adhesion Probability in Fibre Filters*, First World Filtration Congress, Paris.
- Maw, N., Barber, J. R., and Fawcett, J. N. (1977). *Mech. Res. Comm.*, 4:17–22.
- Mindlin, R. D., and Deresiewicz, H. (1953). *J. Appl. Mech.* 75:327–344.
- Reed, J. (1986). *J. Appl. Mech.* 52:229.
- Roberts, A. D., and Thomas, A. G. (1975). *Wear* 33:45–64.
- Rogers, L. N., and Reed, J. (1984). *J. Phys. Ser. D* 17:677–689.
- Rumpf, H. (1990) *Particle Technology*, (F. A. Bull, transl.), Chapman and Hall, London.
- Taylor, J. R. (1982). *An Introduction to Error Analysis*, University Science Books, California.
- Timoshenko, S., and Goodier, J. N. (1951). *Theory of Elasticity*, McGraw-Hill, New York.
- Wall, S., John, W., and Goren, S. (1989). In *Particles on Surfaces 2: Detection Adhesion and Removal* (K. L. Mittal, ed.) Plenum Press, New York.
- Wall, S., John, W., Wang, H.-C., and Goren, S. (1990). *Aerosol Sci. Technol.*, 12:926–946.
- Wang, H.-C., and John, W. (1988). In *Particles on Surfaces 1: Detection Adhesion and Removal*, (K. L. Mittal, ed.), Plenum Press, New York.

Received May 1, 1991; accepted July 10, 1991.